TRANSNAV International Journal on Marine Navigation and Safety of Sea Transportation
Volume 6 Number 4 December 2012

Methods of Iceberg Towing

A. Marchenko & K. Eik
The University Centre in Svalbard, Longyearbyen
STATOIL

ABSTRACT: Mathematical models of iceberg towing by a ship connected to the iceberg by mooring lines are considered. Governing equations describing the towing and the tension of mooring lines in two different schemes of the towing are formulated. Stability of steady solutions describing the towing with constant speed is studied. Numerical simulations are realized to compare results of the modeling with experimental results of model towing in HSVA ice tank.

1 INTRODUCTION

Icebergs may cause a threat to installations, vessels and operations in a number of Arctic and Antarctic regions. If icebergs are detected and considered to be a threat, it has been documented that they can be deflected into a safe direction in approximately 75% of the events (Rudkin et al., 2005). The preferred method for iceberg deflection is single vessel tow rope (Fig 1a). Experimental towing of the iceberg in the Barents Sea was realized with a rope taken around the iceberg by a loop in 2005, and the rope was broken during the towing. Photograph of the towing is shown in Fig. 1.

The majority of the unsuccessful tows ended because the tow slipped over the iceberg while ruptures of tow line or iceberg rolling over are other common explanations (Rudkin et al., 2005). There are also examples of towing where towing in the planned direction was not possible. In order to increase the understanding of what happens when an iceberg tow is started Marchenko and Gudoshnikov (2005) and Marchenko and Ulrich (2008) developed a numerical model for iceberg towing. Eik and Marchenko (2010) analysed results of HSVA experiments on the towing of model iceberg in open water and when broken ice was floating on the water surface. Stability of iceberg towing with floating rope was discussed in (Marchenko, 2010).

Figure 1. Towing of 200000 t iceberg in the Barents Sea.

In the present paper we compare two different methods of iceberg towing, formulate governing

equations, analyse the stability of steady towing and perform numerical simulations of the HSVA experiments on iceberg towing in open water taking into account the influence of natural oscillations of water in the tank.

2 METHODS OF ICEBERGS TOWING

In the practice of iceberg management two methods (I and II) of icebergs towing were performed. In both methods towed iceberg was trapped by a loop of floating synthetics rope ringed around the iceberg. The ends of the rope are fastened on the boat stern in the method I (Fig. 1a) and connected to heavy steel hawser fastened at the boat stern in the method II (Fig. 1b). The rope floats or hangs above the water surface in the method I. In the method II the hawser is submerged and the rope is floating near the iceberg and submerged near its connection to the hawser. Typically the hawser is shorter the rope. In Fig. 2 the line FTR shows floating tow rope and the line W shows the steel hawser. Thin line SS shows the water line around the iceberg and between the iceberg and the boat. In Fig. 2a) the rope segments D_1O_1 and D_2O_2 are floating, and the segments O_1C and O_2C are hanging above water surface. In Fig. 2b) the rope segments O_1B and O_2B are submerged. The realization of the method I is simpler on the practice, but in case of the rope break up the boat stern can be damaged by the rope. In the method II the water takes buffer role in case of the rope break up.

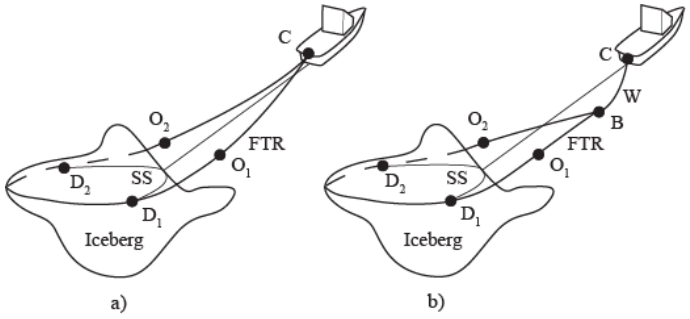

Figure 2. Schemes of iceberg towing with floating (a) (method I) and submerged (b) (method II) tow lines.

The forces applied to the iceberg ($\mathbf{F}_{Ir}$) and to the boat ($\mathbf{F}_{Br}$) by the rope in the method I are calculated with formulas

$$\mathbf{F}_{Ir} = \mathbf{T}_{D1} + \mathbf{T}_{D2}, \quad \mathbf{F}_{Br} = \mathbf{T}_{C1} + \mathbf{T}_{C2}. \qquad (1)$$

The rope tension forces $\mathbf{T}_{D1}$, $\mathbf{T}_{D2}$, $\mathbf{T}_{C1}$ and $\mathbf{T}_{C2}$ are shown in Fig. 3. The forces applied to the iceberg ($\mathbf{F}_{Ir}$) by the rope and to the boat ($\mathbf{F}_{Bh}$) by the hawser in the method II are calculated with formula

$$\mathbf{F}_{Ir} = \mathbf{T}_{D1} + \mathbf{T}_{D2}, \quad \mathbf{F}_{Bh} = \mathbf{T}_{C}. \qquad (2)$$

The rope tension forces $\mathbf{T}_{D1}$, $\mathbf{T}_{D2}$ and $\mathbf{T}_{C}$ are shown in Fig. 4.

Safety requires avoid the approaching of iceberg to the boat. Therefore in both methods of icebergs towing distances X_1 and X_2 shown in Fig. 3 and Fig. 4 should be much greater distances R_1 and R_2. It can be expressed by the inequality $\chi << 1$, where $\chi = R/X$ and R represents iceberg radius. Quantity X represents distance between the boat stern and the points D_1 and D_2, where the rope approaches to the iceberg. Assuming $X \approx 500$ m and representative radius of the iceberg 50 m we find that $\chi = 0.1$. Distances z_C and z_B are typically smaller 10 m. Therefore parameter $\varepsilon = z_{C,B}/l_r$ is smaller 0.02.

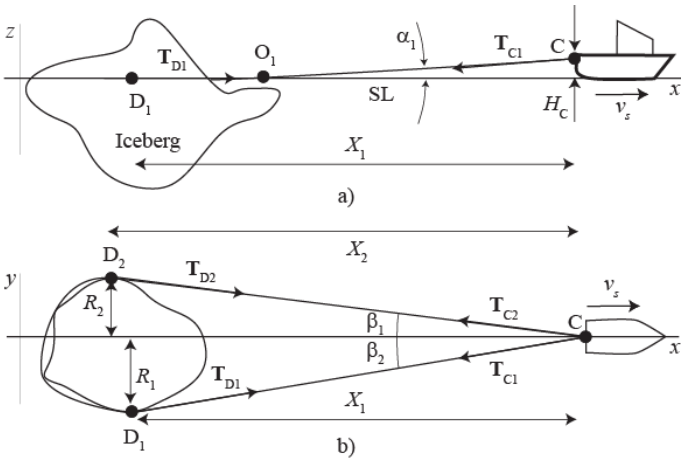

Figure 3. Schemes of towing line in method I in lateral (a) and upward (b) projections.

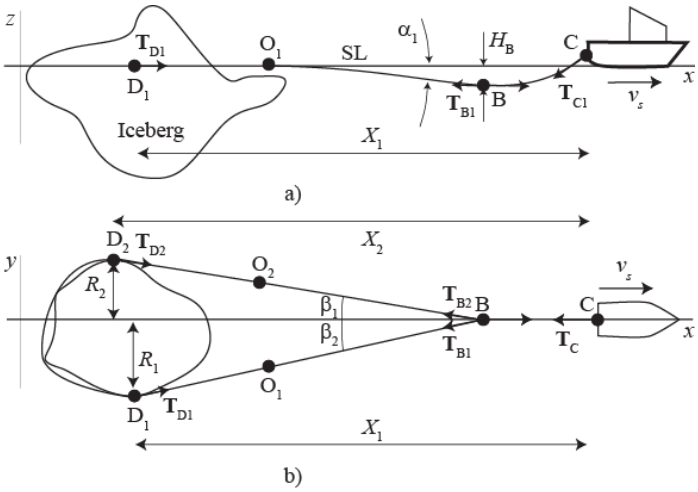

Figure 4. Schemes of towing line in method II in lateral (a) and upward (b) projections.

Angles $\alpha_{1,2}$ and $\beta_{1,2}$ shown in Fig. 3 and Fig. 4 are of the orders ε and χ respectively. Projections of the rope tensions on the x-direction are

proportional to $\cos\alpha_{1,2}$ and $\cos\beta_{1,2}$. Therefore their difference has the order $O(\varepsilon^2, \chi^2)$, and formulas (1) and (2) can be written with accuracy $O(\varepsilon, \chi)$ as follows

$$F_{Ir} = T, \quad F_{Br} = -T, \tag{1a}$$

$$F_{Ir} = T, \quad F_{Bh} = -T_C = -T, \tag{2a}$$

where $T/2$ is the rope tension, F_{Ir}, F_{Br} and F_{Bh} are the absolute values of the forces applied to the iceberg and to the boat along the x-axis.

Further it is assumed that the difference between x-coordinates of the points D_1 and D_2 is much smaller than the iceberg radius R, and $X_1 = X_2 = X$ with accuracy $O(\varepsilon, \chi)$. In this case the rope tension is expressed as a function

$$T = T(X), \quad dT/dX > 0 \tag{3}$$

where X is the distance between points of the rope fastening on the boat stern and on the iceberg surface. Inequality in (3) means that the increase of X is accompanied by the increase of the rope tension.

3 GOVERNING EQUATIONS

Equations of momentum balance for boat and iceberg connected by tow line are written as follows

$$M_s \frac{dv_s}{dt} = -R_s - T + P - M_s g \partial h/\partial x, \tag{4}$$

$$M_i \frac{dv_i}{dt} = -R_i + T - M_i g \partial h/\partial x, \tag{5}$$

where M_s and M_i are the masses of the boat and the iceberg including the added mass, P is the boat propulsion, and $\partial h/\partial x$ is the water surface gradient. It is assumed that horizontal scale of water surface elevation is much greater than the iceberg diameter and ship length. Water resistances to boat motion (R_s) and to iceberg motion (R_i) are described by square low as follows

$$R_s = \rho_w C_{ws} S_s |v_s - u|(v_s - u), \quad R_i = \rho_w C_{wi} S_i |v_i - u|(v_i - u), \tag{6}$$

where S_s is wet surface of the boat hull, and S_i is representative area of vertical cross-section of submerged surface of the iceberg in perpendicular direction to the tow direction, and u is water velocity. Drag coefficients are equal to $C_{ws} = 0.003$ (Voitkunsky, 1988) and $C_{wi} \in (0.5,1)$ (Robe, 1980).

Equations (4) and (5) are completed by the definition of relative velocity as follows

$$\frac{dX}{dt} = v_s - v_i. \tag{7}$$

Equations (4), (5) and (7) perform closed system of ordinary differential equations relatively unknown functions of the time $v_s(t)$, $v_i(t)$ and $X(t)$. They have steady solution describing steady towing with constant speed v_0, constant propulsion P_0, constant water velocity u and $\partial h/\partial x = 0$. For the steady towing it follows

$$v_s = v_i = v_0, \quad T_0 = R_i, \quad R_s + T_0 = P_0, \tag{8}$$

$$v_0 - u = \sqrt{\frac{P_0}{\rho_w (C_{ws} S_s + C_{wi} S_i)}}, \quad T_0 = (v_0 - u)^2 \rho_w C_{wi} S_i \tag{9}$$

Distance $X = X_0$ is determined from the first formula (3) when $T = T_0$.

Dimensionless variables: time t', velocities v'_s and v'_i, rope tension τ, boat propulsion π and distance Z between points of the rope fastening are introduced as follows

$$t' = \frac{t}{t_{r,1}}, \quad v'_s = \frac{v_s}{v_0}, \quad v'_i = \frac{v_i}{v_0}, \quad u' = \frac{u}{v_0}, \quad \tau = \frac{T}{T_0},$$
$$\pi = \frac{P}{P_0}, \quad Z = \frac{X}{l_r}, \tag{10}$$

where $t_{r,1} = M_s v_0 / T_0$ is the representative time, and l_r is the rope length. Equations (4), (5) and (7) are written in dimensionless variables as follows (primes near dimensionless variables are omitted)

$$\frac{dv_s}{dt} = -\varepsilon_1 |v_s - u|(v_s - u) - \tau + (1 + \varepsilon_1)\pi - \varepsilon_w \partial\eta/\partial x, \tag{11}$$

$$\frac{dv_i}{dt} = -\varepsilon_2 |v_i - u|(v_i - u) + \varepsilon_2 \tau - \varepsilon_w \partial\eta/\partial x, \quad \gamma \frac{dZ}{dt} = v_s - v_i,$$

where $\varepsilon_1 = C_{ws} S_s / (C_{wi} S_i)$, $\varepsilon_2 = M_s / M_i$, $\gamma = l_r T_0 / (M_s v_0^2)$, $\varepsilon_w = a / l_r$, and a is the amplitude of water surface elevation. Simple estimates show that $\varepsilon_{1,2} << 1$ when the iceberg is not very small.

Steady solution in dimensionless variables is written as

$$v_s = v_i = \tau = \pi = 1. \tag{12}$$

Value $Z = Z_0$ for steady towing is constructed as solution of the equation $\tau(Z_0) = 1$.

4 STABILITY OF STEADY TOWING

Solution of equations (11) in the vicinity of the steady point is written in the form

$$v_s = 1 + \delta v_s, \quad v_i = 1 + \delta v_i, \quad Z = Z_0 + \delta Z, \tag{13}$$

where new independent variables $\delta v_s(t)$, $\delta v_i(t)$ and $\delta\Sigma(t)$ describe small fluctuations in the vicinity of the steady solution. Substitution of formulas (13) in equations (11) leads to the following equations

$$\frac{d\delta v_s}{dt} = -2\varepsilon_1 \delta v_s - \tau_0' \delta Z, \quad \frac{d\delta v_i}{dt} = -2\varepsilon_2 \delta v_i + \varepsilon_2 \tau_0' \delta Z,$$
$$\gamma \frac{d\delta Z}{dt} = \delta v_s - \delta v_i, \tag{14}$$

where $\tau_0' = d\tau / dZ$ by $Z = Z_0$.

Substituting exponential solution $\delta v_s = \delta v_{s,0} e^{\psi t}$, $\delta v_i = \delta v_{i,0} e^{\psi t}$, $\delta Z = \delta Z_0 e^{\psi t}$, in equations (14) we find that eigenvalues ψ are the roots of the cubic equation

$$F(\psi) \equiv \psi(\psi + 2\varepsilon_1)(\psi + 2\varepsilon_2) + \mu(\psi(1+\varepsilon_2) + 2\varepsilon_2(\varepsilon_1 + \varepsilon_2)) = 0, \tag{15}$$

where $\mu = \tau_0' / \gamma > 0$. Roots $\psi_{i,0}$ of equation (15) by $\varepsilon_1 = \varepsilon_2 = 0$ are chosen as the first approximation of the roots when $\varepsilon_{1,2} << 1$. One finds

$$\psi_{1,0} = 0, \quad \psi_{2,0} = i\sqrt{\mu}, \quad \psi_{3,0} = -i\sqrt{\mu}. \tag{16}$$

Next approximation is expressed by the formulas

$$\psi_1 = -2\varepsilon_2, \ \psi_2 = i\sqrt{\mu} - \varepsilon_1 + \frac{i\sqrt{\mu}}{2}\varepsilon_2,$$
$$\psi_3 = -i\sqrt{\mu} - \varepsilon_1 - \frac{i\sqrt{\mu}}{2}\varepsilon_2. \tag{17}$$

From formulas (17) follows that real parts of eigen-values ψ are negative. Therefore the solution describing steady towing is stable. At the same time absolute values the of real parts of eigen-values ψ_2 and ψ_3 are much smaller than absolute values of their imaginary parts: $\left|\mathrm{Re}(\psi_{2,3})\right| << \left|\mathrm{Im}(\psi_{2,3})\right|$. Therefore damping of perturbations of the steady solution will be accompanied by oscillations with dimensionless frequency $\sqrt{\mu}$. Dimensional period of the oscillations is calculated as follows $t_{p,1} = 2\pi t_{r,1} / \sqrt{\mu}$. Oscillations of mooring system with floating submerged sensors were observed and studied by Hamilton (2000).

5 MODEL TESTS OF ICEBERGS TOWING

Model tests on the iceberg towing were performed at Hamburg Ship Model Basin (HSVA), Germany. Two model icebergs with cylindrical and rectangular shapes were made from water ice and towed using scheme shown in Fig. 1b) in the tank with different concentration of ice floes on the water surface. The description and results of the experimental studies are performed in the paper (Eik and Marchenko, 2010). In the present paper we consider only results of the experiment when cylindrical iceberg was towed in the water with free surface. Dimensions of model iceberg and fragment of the towing are shown in Fig. 5.

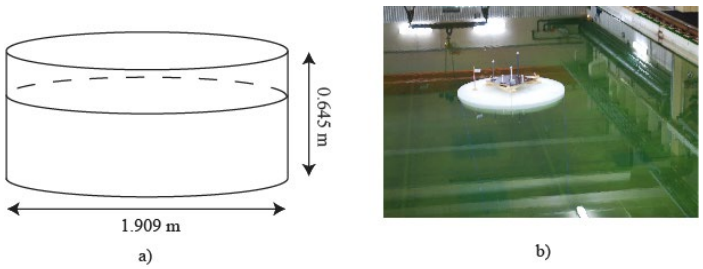

Figure 5. Dimensions of model iceberg (a) and fragment of the HSVA experiment (b).

The movement and rotation of towed icebergs were recorded in all six degrees of freedom with a Qualisys-Motion Capture System. The platform with sensors was installed on the iceberg surface to monitor the iceberg motion as it is visible in Fig. 5b). Three degrees of the movement are characterized by the horizontal distance between the carriage and the sensors (surge), sideways movement between fixed point at the carriage and the sensors (sway), and by the vertical displacement of the sensors (heave). Three degrees of the rotation are performed by the pitch, the roll and the yaw of the platform with sensors with respect to the direction of the tank extension.

The tow line consisted of floating rope Dyneema and steel wire. Characteristics of the towing rope Dyneema and the wire used in the tests are performed in Tables 1 and 2 for model scale. The tension in the tow line was recorded in three locations: on the end of the wire on the carriage and on the rope ends near the point of their connection with the wire (point B in Fig. 5). Some of the loads cells in some of the tests were “drifting” and manually corrected. This causes some unfortunate uncertainties in the load results. Average tow loads were varied in the range from 0.78 N to 4 N in the tests with open water.

The length and the water depth in the tank are equal $L_t = 72$ m and $H_t = 2.5$ m respectively (Fig. 5). Natural oscillations of the water in the tank can influence the towing. Horizontal water velocity u and water surface elevation h of the first natural mode are described by formulas

$$u = u_0 \cos\omega_1 t \sin k_{1x} x, \quad h = h_0 \sin\omega_1 t \cos k_{1x} x, \tag{18}$$

where t is the time, x is the horizontal coordinate directed along the tank, h_0 is the amplitude of water surface elevation and $u_0 = -\omega_1 h_0 /(k_{1x} H_t)$ is the amplitude of water velocity oscillations in the first mode, $k_{1x} = \pi / L_t$ is the wave number, and $\omega_1 = \sqrt{g H_t k_1}$ is the wave frequency. The period T_1 of the first natural mode is calculated with formula

$$T_1 = 2\pi / \omega_1 \approx 29\,\text{s}. \qquad (19)$$

Water surface deformed by the first natural mode of the tank is shown in Fig. 5 by blue dashed and continuous lines at the different phases of the oscillation. Fig. 5 also explains that the distance X between the center of the iceberg and the carriage can be different from the distance X_{cs} between the sensor platform and the carriage because of the natural oscillation of the water in the tank and the iceberg pitch and roll. Difference $X - X_{cs}$ can depend on the sway and the yaw of the iceberg if the position of the sensor platform relatively the iceberg center is determined with insufficient accuracy.

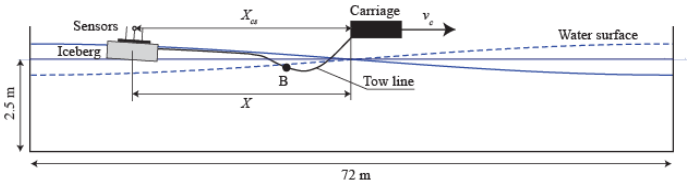

Figure 6. Scheme of the towing in the HSVA tank.

Period of heave oscillations of floating ice cylinder is estimated with the formula

$$T_c = 2\pi\left(\rho_w h_c /(\rho_w - \rho_i) g\right)^{1/2}, \qquad (20)$$

where $\rho_w = 1000\,\text{kg/m}^3$ and $\rho_i = 887\,\text{kg/m}^3$ are water and ice densities, and h_c is the cylinder height. Assuming $h_c = 0.645\,\text{m}$ we find the period of heave oscillation $T_c = 4.8\,\text{s}$ for the iceberg model.

The speed of the carriage in the experiment is shown in Fig. 7a) versus the time Mean tow speed is equal to 0.11 m/s when $125\,\text{s} < t < 250\,\text{s}$, and it is 0.13 m/s when $270\,\text{s} < t < 400\,\text{s}$. t. Fig. 8a) shows the difference between the carriage speed and its moving average calculated over 6 s. The mean deviation of the carriage speed is about 0.005 m/s. The carriage speed doesn't include oscillations with well recognized periodicity. Fig. 7b,c,d) show the surge, sway and heave of the iceberg versus the time. The characteristics of iceberg rotation performed by the pitch, roll and yaw are shown in Fig. 8b,c,d). The surge, sway, roll and yaw have visible correlation due to long term trend changing its direction when $t \approx 200\,\text{s}$. The surge and heave have oscillations with period about 30 s closed to the period T_1 of the first natural mode of the tank.

The amplitude of the heave oscillations varied within 0.5 - 1 cm when the iceberg was near the edge of the tank and decreases to smaller values when the iceberg was towed to the center of the tank. From the first formula (18) it follows that the amplitude of water velocity oscillations in the first mode u_0 is varied from 2 cm/s to 4 cm/s in the middle part of the tank when $h_0 = 0.5 - 1\,\text{cm}$. The decrease of the heave amplitude in Fig. 6d) with the time can relate to the decrease of the amplitude of water surface elevation in the middle part of tank according to the second formula (18).

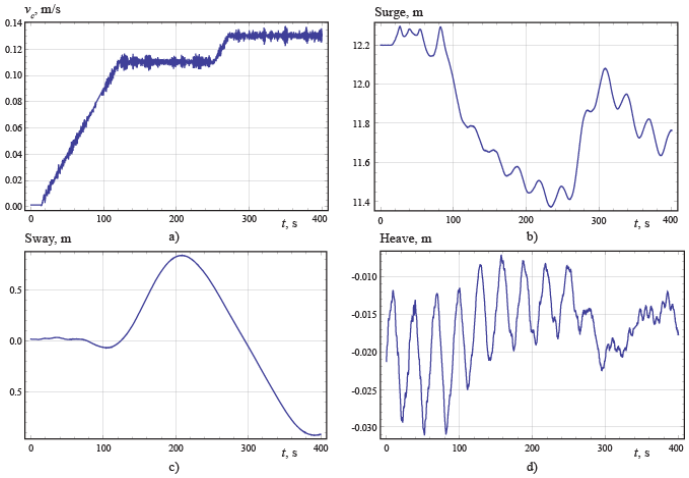

Figure 7. The speed of the carriage (a), horizontal distance between the carriage and the sensors installed on the iceberg (b), sideways movement relative between fixed points at carriage and the sensors (c) and iceberg heave (d) versus the time.

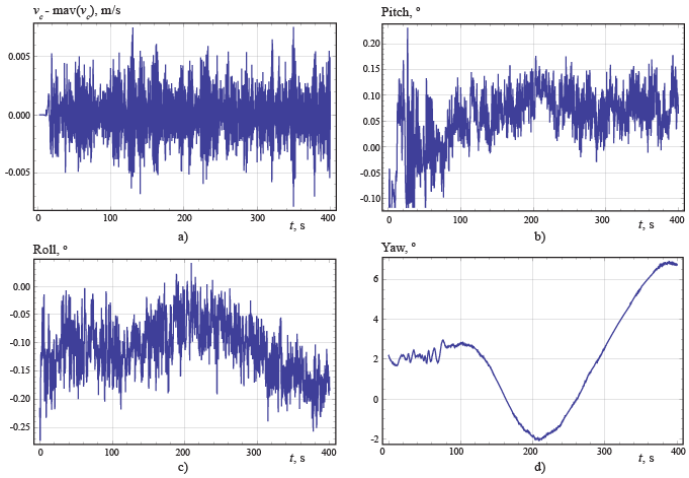

Figure 8. Difference between the carriage speed and its moving average (a), pitch (b), roll (c) and yaw (d) of the iceberg versus the time.

6 RESULTS OF NUMERICAL SIMULATIONS

Characteristics of towing lines in steady towing. Numerical simulations are performed in model and full scales. Properties of the towing rope and the hawser are performed in Tables 1 and 2. Towing

rope Dyneema was used in the HSVA tests. Characteristics of the towing rope Dyneema performed in Table 1 for the full scale are taken from the web-address www.dynamica-ropes.dk. It is assumed that the diameter of the hawser should be the same as the rope diameter since their strengths are almost the same.

Table 1. Tow rope properties (model and full scales)

Property	Unit	Model scale	Full scale
Total length	[m]	23	920
Length CD (Fig. 2)	[m]	10	400
Length BD (Fig. 3)	[m]	10	400
Weight	[Kg/m]	0.0069	6.22
Diameter	[m]	0.004	0.12
E-Module	[GPa]	95	95
Ultimate Load	[T]	1.3	1000

Table 2. Tow hawser properties (model and full scales)

Property	Unit	Model scale	Full scale
Total length	[m]	2.05	82
Weight	[Kg/m]	0.049	79.6
Diameter	[m]	0.003	0.12
E-Module	[GPa]	200	200
Ultimate Load	[T]	-	1000

From formulas (1a) and (2a) it follows that the towing with rope loop around the iceberg can be performed as the towing with one rope having double weight $2W_r$ and double buoyancy force $2W_b$. Models of towing lines related to towing schemes shown in Fig. 1 are performed in the Appendix. Fig. 9 perform the dependence of the rope tension T from the distance $\Delta X = l_{TL} - X$, where l_{TL} is total length of the towing line between the points C and D, in model and full scales. Curves 1 and 2 are related to towing method I and II shown in Fig. 1a) and Fig. 1b) respectively, $l_{TL} = 12.05\,\text{m}$ in model scale and $l_{TL} = 482\,\text{m}$ in full scale. One can see that the slope of the tension curve for the first towing scheme is higher than for the second towing scheme when the tension is relatively high.

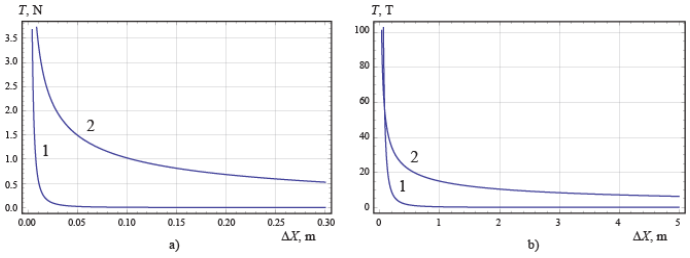

Figure 9. Rope tension T versus distance decreasing ΔX between the boat and the iceberg in model (a) and full (b) scales.

The shape of towing lines in steady towing performed by schemes shown in Fig.1a) and Fig. 1b) are performed in Fig. 10a,b) and Fig. 10c,d) respectively in model and full scales. One can see that all curves in Fig. 10 have small slopes. Thus assumptions made in the Appendix for the construction of the towing lines models are satisfied. It is also visible that towing rope always has floating part. In this case variations of the rope tension influence significantly vertical displacement of the towing lines and have insignificant influence on horizontal displacements of points C, D and B in comparison with the rope length. These displacements are invisible in Fig. 10 and therefore are shown by squares.

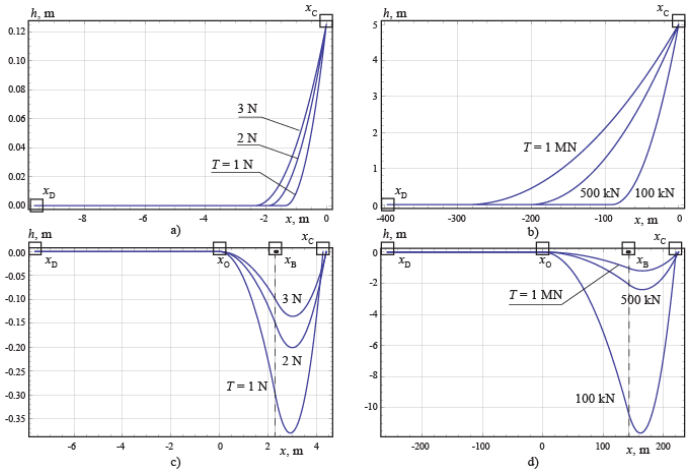

Figure10. The shape of towing lines in steady towing in model (a,c) and full scales (b,d) calculated with different values of the rope tension T.

Oscillations in unsteady towing. Dimensional period of these oscillations is estimated by the formula $t_p = 2\pi t_* / \sqrt{\mu}$, where $t_{r,2} = M_i v_0 / T_0$. Periods t_p are shown in Fig. 11 versus the tow load T in model and full scales. Curves 1 and 2 are related to the towing schemes shown respectively in Fig. 1a) and Fig. 1b). The periods are decreased with the increasing of the tow load. Representative value of the period is few tens of seconds when the towing is occurred according to Fig. 1b). Periods of oscillations in the towing scheme in Fig. 1a) are smaller 10 sec in model scale and 20 sec in full scale when tow load is relatively high. Periods of oscillations in the towing scheme in Fig. 1b) are higher then in the towing scheme in Fig. 1a) . From Fig. 11a) follows that period t_p is closed to period T_1 of the first natural mode of the tank, when the rope tension is about 2 N. It can create resonance effect. In full scale period t_p can be closed to swell period. For the conditions of the Barents Sea swell period is about 12 s. From Fig. 10b) it follows that the swell period can be closed to the period T_1 when the towing is performed according to the scheme in Fig. 1a).

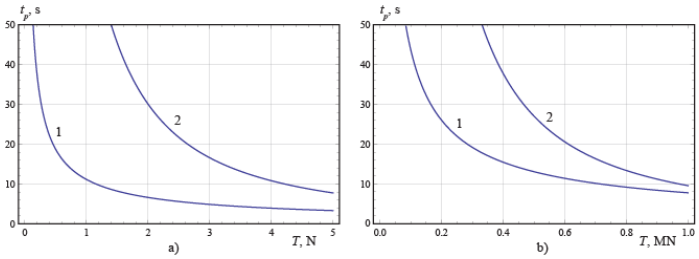

Figure 11. Periods of oscillations in model (a) and full (b) scales.

Fig. 12a,c) show the data measured in the experiment on the towing of model iceberg with cylindrical shape in the HSVA tank (Eik and Marchenko, 2010). Iceberg diameter and height are 1.909 m and 0.645 m. The towing was realized as it is shown in Fig. 1b). Characteristics of tow line are shown in Tables 1, 2. The rate of the distance between the carriage and iceberg (dX/dt) is calculated using the experimental data. The iceberg motion was calculated using equations (11), where v_s was substituted equaling to the carriage velocity $v_c(t)$. Initial conditions were $v_i = 0$ and $Z = 1.19$ by $t = 0$. It is assumed that $v_0 = 0.11\,\text{m/s}$, $M_i = 1643\,\text{kg}$ and $T_0 = 2.34\,\text{N}$. Figure 13a) shows carriage velocity used in numerical simulations. Computed displacement of the iceberg is shown in Fig. 13b). Fig. 13a) shows surge rate dX/dt calculated using experimental data. Fig. 13b) shows the surge rate without accounting of the natural oscillations of the water in the tank. Figures 13c) and Fig. 13d) shows the surge rate with accounting of the natural oscillations with period 29 s and 16 s respectively. One can see that periods and amplitudes of oscillations of dX/dt in Fig. 13a) are most close to those performed in Fig. 13c).

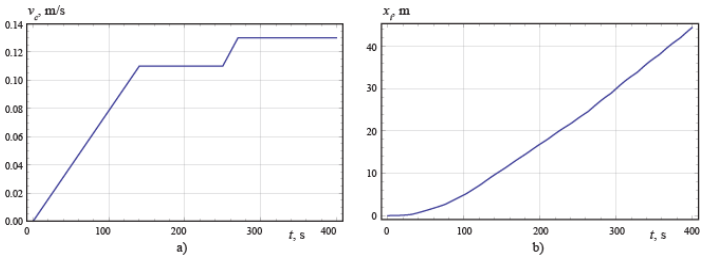

Figure 12. Carriage velocity versus the time used in simulations (a). Calculated iceberg displacement versus the time (b).

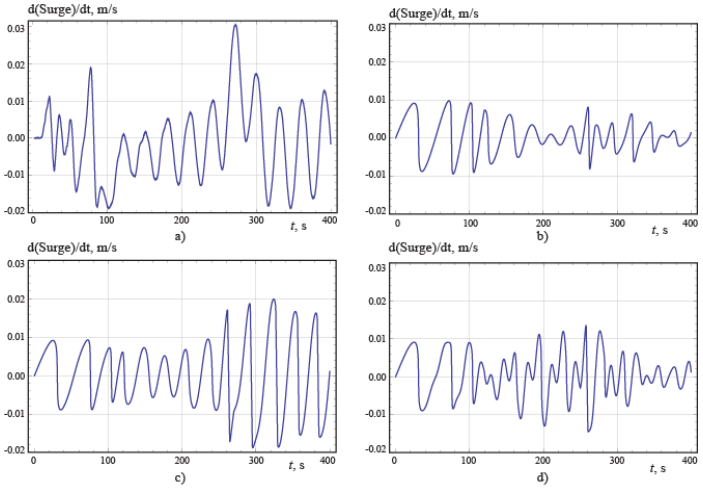

Figure 13. Surge rates calculated with experimental data (a), with numerical simulations without accounting of natural oscillations of the water in the tank (b) and with accounting of natural oscillations of the water in the tank with periods 29 s (c) and 16 s (d).

CONCLUSIONS

Stability of steady towing of iceberg is analyzed for two methods of the towing (Fig. 2). It is shown that steady towing is stable, but damping of steady towing perturbations is accompanied by oscillations in the system ship-tow line-iceberg. The resonance of these oscillations with swell of 12 s period observed in the Barents Sea is available when the towing is realized with floating tow line (method I). Model experiments on iceberg towing were performed in HSVA ice tank. Surge and heave oscillations of model icebergs were observed in the experiments. Periods of these oscillations were close to the period of the first natural mode of water oscillations in the tank 29 s. Numerical simulations confirm that the amplitudes of surge and heave oscillations of iceberg models were influenced by the natural oscillations of the water in the tank.

REFERENCES

Eik, K., Marchenko, A., 2010. Model tests of iceberg towing. Cold Regions Science and Technology, 61, pp. 13-28.

Hamilton, J.M., 2000. Vibration-based technique for measuring the elastic properties of ropes and the added masses of submerged objects. J. of Atmospheric and Oceanic Technology. Vol. 17, pp. 688-697.

Marchenko, A., Gudoshnikov, Yu., 2005. The Influence of Surface Waves on Rope Tension by Iceberg Towing. Proc. of 18th Int. Conference on Port and Ocean Engineering under Arctic Conditions (POAC'05), Vol. 2, Clarkson University, Potsdam, NY, pp.543-553.

Marchenko, A., and C., Ulrich, 2008. Iceberg towing: analysis af field experiments and numerical simulations. Proceedings of 19th IAHR International Symposium on Ice "Using New Technology to Understand Water-Ice Interaction", Vancouver, BC, Canada, July 6-11, 2008, Vol.2, 909-923.

Marchenko, A.V., 2010. Stability of icebergs towing. Transactions of the Krylov Shipbuilding Research Institute. Marine Ice Technology Issue. 51 (335), 69-82. ISBN 0869-8422. (in Russian)
McClintock, J., McKenna, R. and Woodworth-Lynas, C. (2007). Grand Banks Iceberg Management. PERD/CHC Report 20-84, Report prepared by AMEC Earth & Environmental, St. John's, NL, R.F. McKenna & Associates, Wakefield, QC, and PETRA International Ltd., Cupids, NL., 84 p.
Robe, R.Q., 1980. Iceberg drift and deterioration. In: Colbeck, S. (Ed.), Dynamics of Snow and Ice Masses. Academic Press, New York. pp. 211-259.
Rudkin, P., Boldrick, C. and Barron Jr., P., 2005. PERD Iceberg Management Database. PERD/CHC Report 20-72, Report prepared by Provincial Aerospace Environmental Services (PAL), St. John's, NL., 71 p.
Voitkunsky J.I., 1988. Resistance to ship motion. Leningrad: Sudostroenie. 287 p. (in Russian)

APPENDIX

Model of the towing with floating rope

The scheme of icebergs towing with floating rope is shown in Fig. 14a). The rope segment OC hangs in the air, and the rope segment OD floats on the water surface. The coordinate of the point O is equal to $-x_{\mathrm{O}}$, and the coordinate of point D is equal to $-X$. The rope is fastened to the boat stern in the point C with coordinates $x=0$ and $z=z_{\mathrm{C}}$. The motion of the rope is occurred under the influence of the gravity force, the rope tension and the rope inertia. Momentum balance of the rope segment hanging in the air with length ds is written as follows

$$\frac{W}{g}\mathbf{a}=\frac{d}{ds}\mathbf{T}+\mathbf{W}, \qquad (\Pi 1)$$

where $\mathbf{W}=(0,-W_r)$ is the weight of the rope of unit length, $\mathbf{T}$ is the rope tension, $\mathbf{a}$ is the acceleration (Fig. 14c). Since the vector of the rope tension is tangential to the rope it can be performed as $\mathbf{T}=T\boldsymbol{\tau}$, where $\boldsymbol{\tau}$ is the tangential vector of unit length to the rope segment ds. Using Frenet formulas equation (П1) is written in the form

$$\frac{W}{g}\mathbf{a}=\frac{dT}{ds}\boldsymbol{\tau}-Tk\mathbf{n}+\mathbf{W}, \qquad (\Pi 2)$$

where $\mathbf{n}$ is unit normal vector to the rope segment ds and k is the rope curvature.

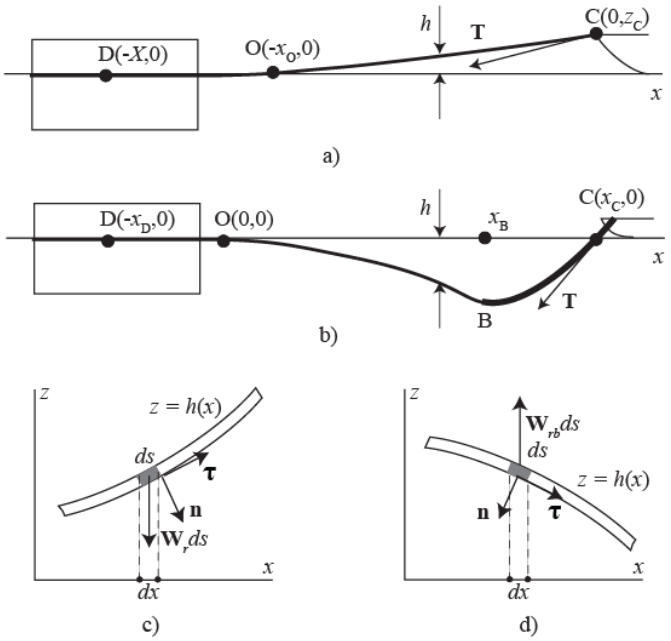

Figure 14. Schemes of iceberg towing with floating (a) and submerged (b) ropes. Schemes of forces applied to the rope hanging in the air (c) and to submerged rope (b).

The shape of the hanging rope is described by equation $z=h(x,t)$, where x and z are the horizontal and vertical coordinates and t is the time. The rope curvature is calculated by the formula $k=\left(\partial^2 h/\partial x^2\right)\left(1+\left(\partial h/\partial x\right)^2\right)^{-3/2}$. In static case the integration of the projection of equation (П2) on tangential vector $\boldsymbol{\tau}$ leads to the formula $T=T_{st}+W_r h$, where T_{st} is a constant. The projection of equation (П2) on normal vector $\mathbf{n}$ is written as follows

$$T\frac{d^2h}{dx^2}=W_r\sqrt{1+\left(\frac{dh}{dx}\right)^2}, \qquad (\Pi 3)$$

Dimensionless variables are introduced by formulas

$$\varsigma=\frac{x}{l_{r,0}},\ \tau=\frac{T_{st}}{T_0},\ \eta=\frac{h}{z_{\mathrm{C}}}, \qquad (\Pi 4)$$

where $l_{r,0}$ is the rope length and T_0 is the rope tension in steady towing. In dimensionless variables equation (П3) has the following form

$$(\tau+\upsilon\eta)\frac{\varepsilon}{\upsilon}\frac{d^2\eta}{d\varsigma^2}=\sqrt{1+\left(\varepsilon\frac{d\eta}{d\varsigma}\right)^2}, \qquad (\Pi 5)$$

where dimensionless coefficients ε and υ are introduced as follows

$$\varepsilon=\frac{z_{\mathrm{C}}}{l_r},\ \upsilon=\frac{W_r z_{\mathrm{C}}}{T_0}. \qquad (\Pi 6)$$

The rope tension T_0 is estimated with formula (8). Assuming $z_C = 10\,\mathrm{m}$, $W_r = 50\,\mathrm{Nm^{-1}}$, $S_0 = 10^3\,\mathrm{m}^2$, $C_{wi} = 0.6$ and $v_0 = 0.5\,\mathrm{ms^{-1}}$ we find that $T_0 = 150\,\mathrm{kN}$ and $\upsilon \approx 0.033$.

With accuracy up to high order terms equation (П3) is written in dimensionless variables (П4) as follows

$$\frac{d^2\eta}{d\varsigma^2} = \frac{k_r}{\varepsilon\tau},\ \varsigma \in (-\varsigma_O, 0). \qquad (П7)$$

where $k_r = l_r W_r / T_0$ and τ is dimensionless rope tension.

Boundary conditions for equation (П7) are formulated as follows

$$\eta = 1,\ \varsigma = 0, \qquad (П8)$$

$$\eta = 0,\ \frac{d\eta}{d\varsigma} = 0,\ \varsigma = -\varsigma_O. \qquad (П9)$$

From (П8) and (П9) it follows

$$\eta = \frac{k_r \varsigma}{\varepsilon\tau}\left(\frac{\varsigma}{2} + \varsigma_O\right) + 1,\ \varsigma \in (-\varsigma_O, 0), \qquad (П10)$$

$$\tau = \frac{k_r \varsigma_O^2}{2\varepsilon}. \qquad (П11)$$

Dimensionless length of the rope segment hinging in the air is calculated from the formula

$$l_{OC} = \int_{-\varsigma_O}^{0} \sqrt{1 + \varepsilon^2\left(\frac{d\eta}{d\varsigma}\right)^2}\, d\varsigma = \int_{-\varsigma_O}^{0} \left(1 + \frac{\varepsilon^2}{2}\left(\frac{d\eta}{d\varsigma}\right)^2\right) d\varsigma + O(\varepsilon^4), \qquad (П12)$$

and total length of the rope is equal to

$$1 = l_{OC} + Z - \varsigma_O. \qquad (П13)$$

From formula (П12) it follows

$$l_{OC} = \varsigma_O\left(1 + \frac{2\varepsilon^2}{3\varsigma_O^2}\right). \qquad (П14)$$

From formulas (П13) and (П14) follows

$$\varsigma_O = \frac{2\varepsilon^2}{3(1-Z)}. \qquad (П15)$$

Substituting (П15) in formula (П11) we find the expression of the rope tension

$$\tau = \frac{2k_r\varepsilon^3}{9(1-Z)^2}. \qquad (П16)$$

In the steady towing $\tau = 1$ and $Z_0 = 1 - \sqrt{2\varepsilon k_r}/3$. Dimensionless parameter $\mu = \tau_0'/\gamma$ is calculated with the formula

$$\mu = \frac{3\sqrt{2}}{\gamma\varepsilon\sqrt{\varepsilon k_r}}. \qquad (П17)$$

Formula (П16) is applicable when $\varsigma_O \le Z$. This condition imposes limitation for the tension $\tau \le \tau_{cr}$, where $\tau_{cr} = k_r/(2\varepsilon^2)$. The rope hangs above the water when $\tau > \tau_{cr}$. Dimensional value of critical rope tension $T_{cr} = l_r W_r/(2\varepsilon^2) \approx 1632\,\mathrm{T}$, when $l_r = 400\,\mathrm{m}$, $z_C = 10\,\mathrm{m}$, $W_r = 50\,\mathrm{Nm^{-1}}$. This value is much greater the strength of synthetic ropes.

Model of the towing with submerged rope

Scheme of iceberg towing with submerged rope is shown in Fig. 14b). The rope is fastened on iceberg surface behind the point D, it is floating between points D and O and submerged between points O and B. The rope BD is connected to the wire BC fastened at the boat stern. The length of the rope between the points C and D is equal l_r, and the length of the wire between the points B and C is equal to l_w. It is convenient to set up the origin in the point O. The coordinates of the points D, O, B and C are equal to $(-x_D, 0)$, $(0,0)$, $(x_B, -z_B)$ and $(x_C, 0)$ respectively. It is assumed that the weight of the rope with unit length is equal to W_r, and it is smaller than the buoyancy force W_b applied to the rope. Therefore the resulting force $W_{rb} = W_b - W_r$ is upward directed (Fig. 14d). The weight of the wire W_w with unit length is much greater the buoyancy force applied to the wire, therefore the influence of the buoyancy force is ignored.

Analogically (П7) the shape of submerged rope OB is described in dimensionless variables by the equation

$$\frac{d^2\eta}{d\varsigma^2} = -\frac{k_{rb}}{\tau},\ \varsigma \in (0, \varsigma_B), \qquad (П18)$$

where $k_{rb} = l_r W_{rb}/T_0$ and τ is dimensionless tension of the rope and the wire. Since z_B is unknown quantity depending on the solution dimensionless variable η is determined by formula $\eta = h/l_r$ in contrast with last formula (П4). Nevertheless further it is assumed that $|d\eta/d\varsigma| << 1$.

Boundary conditions in the point O for the construction of the solution of equation (П18) describing the shape of the rope BD are formulated as follows

$$\frac{d\eta}{d\varsigma} = \eta = 0\,,\ \varsigma = 0 \qquad (\Pi 19)$$

From (П18) and (П19) it follows

$$\eta = -\frac{k_{rb}}{2\tau}\varsigma^2,\ \ \varsigma \in (0, \varsigma_{\mathrm{B}})\,. \qquad (\Pi 20)$$

The shape of the wire BC is described by the equation

$$\frac{d^2\eta}{d\varsigma^2} = \frac{k_w}{\tau},\ \varsigma \in (\varsigma_{\mathrm{B}}, \varsigma_{\mathrm{C}})\,, \qquad (\Pi 21)$$

where $k_w = l_r W_w / T_0$. The solution of equation (П21) satisfying to the condition $\eta = 0$ by $\varsigma = \varsigma_{\mathrm{C}}$ is written as follows

$$\eta = \frac{k_w}{2\tau}(\varsigma - \varsigma_{\mathrm{C}})(\varsigma + B)\,. \qquad (\Pi 22)$$

Matching conditions for solutions (П20) and (П22) have the form

$$\lim_{\varsigma \to \varsigma_{\mathrm{B}} - 0} \eta = \lim_{\varsigma \to \varsigma_{\mathrm{B}} + 0} \eta,\ \ \lim_{\varsigma \to \varsigma_{\mathrm{B}} - 0} \frac{d\eta}{d\varsigma} = \lim_{\varsigma \to \varsigma_{\mathrm{B}} + 0} \frac{d\eta}{d\varsigma}. \qquad (\Pi 23)$$

Analogically (П12) dimensionless unit length of the rope between the points D and B and the wire length between the points B and C are expressed by formulas

$$l_{\mathrm{DB}} = \int_{-\varsigma_{\mathrm{D}}}^{\varsigma_{\mathrm{B}}} \left(1 + \frac{1}{2}\left(\frac{d\eta}{d\varsigma}\right)^2\right) d\varsigma = 1,$$

$$l_{\mathrm{BC}} = \int_{\varsigma_{\mathrm{B}}}^{\varsigma_{\mathrm{C}}} \left(1 + \frac{1}{2}\left(\frac{d\eta}{d\varsigma}\right)^2\right) d\varsigma = \lambda_{wr}\,, \qquad (\Pi 24)$$

Where dimensionless length of the wire in equal to the ratio or dimensional lengths of the wire and the rope (l_w and l_r): $\lambda_{wr} = l_w / l_r$.

Dimensionless distance between the boat and the iceberg is introduced by the formula

$$Z = \varsigma_{\mathrm{D}} + \varsigma_{\mathrm{C}}\,. \qquad (\Pi 25)$$

Formulas (П20), (П22) and conditions (П23) - (П25) are used to perform implicit dependence between dimensionless rope and wire tension τ and distance Z. After simple algebra the implicit dependence is reduced to algebraic equations

$$\beta\varsigma_{\mathrm{C}} + \frac{\alpha\varsigma_{\mathrm{C}}^3}{\tau^2} = \lambda_{wr},\ \ Z - \beta\varsigma_{\mathrm{C}} + \frac{\delta\varsigma_{\mathrm{C}}^3}{\tau^2} = 1\,, \qquad (\Pi 26)$$

where coefficients α, β and δ are expressed by formulas

$$\alpha = \frac{\beta k_w^2}{6}\left(\beta^2 + 3(1-\beta)^2\left(\frac{k_{rb}}{k_w}\right)^2 - 3\beta(1-\beta)\frac{k_{rb}}{k_w}\right),$$

$$\beta = \sqrt{\frac{k_{rb}}{k_{rb} + k_w}},\ \ \delta = \frac{k_{rb}^2(1-\beta)^3}{6}. \qquad (\Pi 27)$$

Excluding ς_{C} from equations (П26) we find explicit formula for the rope tension

$$\tau = \sqrt{\frac{\alpha\varsigma_{\mathrm{C}}^3}{\lambda_{wr} - \beta\varsigma_{\mathrm{C}}}},\ \ \varsigma_{\mathrm{C}} = \frac{\lambda_{wr}\delta - \alpha(1-Z)}{\beta(\alpha + \delta)}. \qquad (\Pi 28)$$

Tension $\tau \to \infty$ when $Z = 1 + \lambda_{wr}$ or when $X = l_r + l_w$ in dimensional variables.

In steady solutions $\tau = 1$ and rope characteristics in steady towing ς_{C}^0 and Z_0 are determined as follows

$$\beta\varsigma_{\mathrm{C}}^0 + \alpha\left(\varsigma_{\mathrm{C}}^0\right)^3 = \lambda_{wr},\ \ Z_0 = 1 + \beta\varsigma_{\mathrm{C}}^0 - \delta\left(\varsigma_{\mathrm{C}}^0\right)^3. \qquad (\Pi 29)$$

Taking differential from equations (П26) in the vicinity of $\tau = 1$ we find

$$\tau_0' = \frac{\beta + 3\alpha\left(\varsigma_{\mathrm{C}}^0\right)^2}{2\beta(\alpha + \delta)\left(\varsigma_{\mathrm{C}}^0\right)^3}\,. \qquad (\Pi 30)$$

Dimensionless parameter μ characterizing the stability of steady towing is calculated with formula $\mu = \tau_0' / \gamma$.